International Journal of Fluid Machinery and Systems
Vol. 6, No. 1, January-March 2013

DOI: http://dx.doi.org/10.5293/IJFMS.2013.6.1.018
ISSN (Online): 1882-9554

Original Paper

Design and Experimental Studies of Radial-Outflow Type Diagonal Flow Fan

Yoichi Kinoue[1], Norimasa Shiomi[1] and Toshiaki Setoguchi[2]

[1]Department of Mechanical Engineering, Saga University
1, Honjo, Saga, 840-8502, Japan, kinoue@me.saga-u.ac.jp
[2]Institute of Ocean Energy, Saga University
1, Honjo, Saga, 840-8502, Japan, setoguci@me.saga-u.ac.jp

Abstract

In order to apply the design method of diagonal flow fan based on axial flow design to the design of radial-outflow type diagonal flow fan which has lower specific speed of 600-700 [min^{-1}, m^3/min, m], radial-outflow type diagonal flow fan which specific speed was 670 [min^{-1}, m^3/min, m] was designed by a quasi three-dimensional design method. Experimental investigations were conducted by fan characteristics test, flow surveys by a five-hole probe and a hot wire probe. Fan characteristics test agreed well with the design values. In the flow survey at rotor outlet, the characteristic region was observed. Two flow phenomena are considered as the cause of the characteristic region, one is tip leakage vortex near rotor tip and another is pressure surface separation on the rotor blade.

Keywords: Diagonal flow fan, Radial outflow, Five-hole probe, Hot wire probe

1. Introduction

A diagonal flow fan has intermediate characteristics between an axial fan and a centrifugal fan. Therefore, there are two ways for the design method of diagonal flow fan, that is, one is the method based on axial flow design and another is the method based on centrifugal flow design. About the design method based on axial flow design, Inoue et al. [1, 2] have proposed a quasi three-dimensional design method of diagonal flow fans. In their method, a three-dimensional flow is divided into two two-dimensional flows, i.e., one is a meridional flow and another is a blade-to-blade flow. In the blade-to-blade flow, the blade profiles selected based on the experimental cascade data are corrected so as to consider the effect of a stream surface inclination and a velocity change of axial flow. Modified NACA65 series carpet diagram [3] was adopted for the selection of blade element in their study. This design method has been verified to be useful for the axial-outflow type diagonal flow fan which has high specific speed around 1200-1600 [min^{-1}, m^3/min, m]. Kaneko et al. [4] and Furukawa et al. [5] have shown the validity of this design method for axial-outflow type diagonal flow fans which have large specific speed. Recently, Maeda et al. [6] and Sawamura et al. [7] have shown that this design method is useful for the axial-outflow type mixed flow pumps of high specific speed.

Nowadays, a combination of a centrifugal fan and a scroll is often used for industrial fans for the specific speed of 600-700 [min^{-1}, m^3/min, m], due to its economical advantage, that is, it is inexpensive to manufacture them by metal sheets. On the other hand, more efficient fans are expected by adopting a diagonal flow fan instead of a centrifugal fan because a diagonal flow fan can be designed by utilizing the design method mentioned above which can attain higher efficiency than centrifugal flow fan.

The objective of this study is to apply the design method of diagonal flow fan based on axial flow design to the design of radial-outflow type diagonal flow fan which has lower specific speed of 600-700 [min^{-1}, m^3/min, m]. The diagonal flow fan of 670 [min^{-1}, m^3/min, m] of specific speed was designed by using the quasi three-dimensional design method of Inoue et al. [1, 2]. In this paper, experimental investigations were conducted for fan characteristics, internal flow surveys by five-hole probe and hot wire probe as well as the design of radial-outflow type diagonal flow fan.

2. Design of Diagonal Flow Fan

Table 1 shows the specifications of fan in this study. The inclination angles of hub and casing are comparably larger values of 50 deg. and 45 deg. so as to fit the radial-outflow for scroll application.

Received March 8 2012; revised June 29 2012; accepted for publication August 26 2012: Review conducted by Prof. Youn-Jea Kim. (Paper number O12004K)
Corresponding author: Yoichi Kinoue, Professor, kinoue@me.saga-u.ac.jp

The quasi three-dimensional design method of Inoue et al. [1, 2] is used to design a diagonal flow fan. Figure 1 shows the design procedure of blade element for a diagonal flow fan. Firstly, a meridional flow is calculated repeatedly so as to get the equilibrium in the q direction (quasi normal direction to a meridional flow) by using Novak's procedure [8]. Figure 2 shows the meridional streamlines calculated, where LE and TE show the leading edge and the trailing edge of rotor, respectively. Secondly, calculated stream surfaces are transformed conformally and blade elements are selected by the experimental two-dimensional cascade data. Modified NACA65 series carpet diagram [3] is adopted for the selection of blade element. The blade profiles selected are corrected so as to consider the effect of a stream surface inclination and a velocity change of axial flow. Finally, the blade profiles corrected on the conformal plane are projected on the original stream surface. Figure 3 shows the perspective views of rotor blade geometry.

3. Experimental Apparatus and Procedure

Figure 4 shows the experimental apparatus used in this study. The flow rate was controlled by setting the damper at downstream of rotor flow. Six porosities are set for the dampers to vary the flow rate. The flow rate was measured by the inlet nozzle. The total pressure increase was measured by a total pressure tube at downstream of rotor flow ($P_{3(t)}$ in Fig. 4). The shaft torque was measured by a torque meter.

Figure 5 shows the outline of fan. In this study, the internal flow of diagonal flow fan without scroll was investigated so as to suppose that the flow field is symmetry in terms of rotating axis, although the diagonal flow fan is designed for scroll type fan. Therefore, the outflow of air is fully radial and symmetrical. The tip clearance of rotor is 0.75 mm.

The measurements of internal flow were conducted by using a five-hole probe and a hot wire probe. Both probes were calibrated in advance. For the hot wire survey, phase locked values were measured by using phase-locked averaging technique [9].

4. Experimental Results and Discussions

4.1 Fan characteristics

Figure 6 shows the characteristic curves of the test fan. Efficiency η, energy coefficient ψ and power coefficient τ are plotted against flow coefficient ϕ. These values are defined as follows.

$$\phi = Q/\left(AU_t\right) \tag{1}$$

$$\psi = \Delta P/\left(\rho U_t{}^2/2\right) \tag{2}$$

$$\tau = T\omega/\left(\rho U_t{}^3 A/2\right) \tag{3}$$

$$\eta = \phi\psi/\tau \tag{4}$$

where, A is the referential area and the reference velocity U_t is defined by the speed of rotor at its tip.

For the curve of energy coefficient ψ, the experimental value agrees well with the design value at design flow rate, and the stall characteristic region is very small in the low flow rate case. For the curve of efficiency η, the profile around the design flow rate is comparably flat and the maximum value of η is about 90 %. For the curve of power coefficient τ, the profile is almost flat for wide range of flow rate, which is preferable for the motor specification.

The experimental result of fan characteristics shows that this diagonal flow fan has high performance and stable characteristics.

4.2 Flow survey results by using five-hole probe

Figure 7 and Fig. 8 show the flow survey results by using five-hole probe at rotor inlet and outlet. Fig. 7(a) and Fig. 8(a) show the meridional velocity V_{mer}, Fig. 7(b) and Fig. 8(b) show the tangential velocity V_θ and Fig. 7(c) and Fig. 8(c) show the total pressure P_T, respectively. In the figures, the radius r is normalized by the radii at hub r_h and at casing r_c, and the velocities are normalized by the reference velocity U_t. The solid lines in the figures show the design values at design flow rate of ϕ=0.265.

In the meridional velocity distribution of Fig. 7(a), the values of V_{mer} decrease near the tip because of the boundary layer in the inlet duct. In the tangential velocity distribution of Fig. 7(b), the values of V_θ is almost zero because of no pre-swirl in this fan. In the total pressure distribution of Fig. 7(c), the values of P_T is almost zero, but the values of P_T decrease near the tip because of the boundary layer in the inlet duct. In the Figures 7(a), 7(b) and 7(c), the values at ϕ=0.276 almost agree with the design values.

In the meridional velocity distribution of Fig. 8(a), the values of V_{mer} decrease both near the hub and near the tip. The decrease near the hub is the effect of boundary layer along the hub and the decrease near the tip is considered as the effect of blockage of the tip leakage vortex, which is because the aspect ratio is comparably low in this fan geometry. The values of V_{mer} at ϕ=0.276 almost agree with the design values at mid span. In the case of low flow rate, the values of V_{mer} increase near the tip, which shows that the flow pattern changes in the case of low flow rate.

In the tangential velocity distribution of Fig. 8(b), the values of V_θ largely increase near the tip, which is considered as the effect of tip leakage vortex as well as Fig. 8(a). The values of V_θ at ϕ=0.276 almost agree with the design values at mid span.

In the total pressure distribution of Fig. 8(c), the values of P_T are almost flat in the case of high flow rate, whereas the values of P_T largely increase near the tip in the case of low flow rate, which is considered as the effect of tip leakage vortex as well as Fig. 8(a) and Fig. 8(b).

4.3 Flow survey results by using hot wire probe

In order to investigate the blade-to-blade flow at rotor outlet, flow surveys were conducted by using a hot wire probe. Six figures from Fig. 9 to Fig. 14 show contour maps of flow survey results at ϕ=0.399 in Fig. 9, ϕ=0.355 in Fig. 10, ϕ=0.276 in Fig. 11, ϕ=0.215 in Fig. 12, ϕ=0.169 in Fig. 13 and ϕ=0.139 in Fig. 14, respectively. In each figure, figure (a) shows the meridional velocity V_{mer} and figure (b) shows the tangential velocity V_{θ}, which are normalized by the reference velocity U_t. The flow is observed from downstream, the solid line shows the trailing edge of rotor blade, and the blade rotates clockwise in the figures, and SS and PS mean the suction surface and the pressure surface of the rotor blade.

In the figures from Fig. 9 to Fig. 14, the location of the characteristic region in the circumferential direction, where the meridional velocity decreases and the tangential velocity increases, can be clearly observed. The region where the meridional velocity decreases and the tangential velocity increases is merely called the characteristic region in the following.

At ϕ=0.276 in Fig. 11 which is near the design value of 0.265, the area of the characteristic region is the smallest among six cases, and, the characteristic region locates almost at the center between the blades in the tip side. When the value of ϕ is reduced, i.e., at ϕ=0.215 in Fig. 12, at ϕ=0.169 in Fig. 13 and at ϕ=0.139 in Fig. 14, the area of the characteristic region spreads circumferentially, and the location of the characteristic region moves toward the suction surface of the rotor blade in the tip side. When the value of ϕ is increased, i.e., at ϕ=0.355 in Fig. 10 and at ϕ=0.399 in Fig. 9, the area of the characteristic region spreads radially, and the location of the characteristic region moves toward the pressure surface of the rotor blade in the tip side.

The cause of the characteristic region is mainly considered as the tip leakage vortex of the rotor from in Fig.11 to in Fig.14. But the pressure surface separation of the rotor blade can be considered as another cause of the characteristic region because the area of the characteristic region become quite large over the full span in the case of high flow rate in Fig. 9 and in Fig. 10. The detailed clarification of the flow phenomena causing the characteristic region should be further investigated both experimentally and numerically.

5. Conclusion

Radial-outflow type diagonal flow fan which specific speed is 670 [min^{-1}, m^3/min, m] is designed by a quasi three-dimensional design method. Experimental investigations were conducted by fan characteristics test, flow surveys by a five-hole probe and a hot wire. Conclusions are summarized as follows.

(1) Experimental results of fan characteristics test agree well with the fan specifications. Flow survey results by the five-hole probe also show the agreement between the designed flow and the experimental flow results.

(2) In the measurement at rotor outlet by using five-hole probe, the decrease of the meridional velocity and the increase of the tangential velocity are observed near the rotor tip.

(3) In the measurement at rotor outlet by using the hot wire probe, the location of the characteristic region in the circumferential direction, where the meridional velocity decreases and the tangential velocity increases, can be clearly observed.

(4) The characteristic region locates almost at the center between the blades at the flow coefficient of 0.276. In the case of low flow rate, the location of the characteristic region moves toward the suction surface of the rotor blade, whereas it moves toward the pressure surface of the rotor blade in the case of high flow rate.

(5) The cause of the characteristic region is mainly considered as the tip leakage vortex of the rotor. But the pressure surface separation is considered as another cause of it in the case of high flow rate.

(6) The detailed clarification of the flow phenomena causing the characteristic region should be further investigated both experimentally and numerically. Casing wall unsteady pressure measurement around rotor is being investigated and steady, three-dimensional Navier-Stokes numerical simulation is being conducted in order to clarify the flow structure in the characteristic region.

Acknowledgments

The authors wish to acknowledge the cooperation to Dr. K. Kaneko, Honorary Professor of Saga University. Also, authors sincerely acknowledge the support for the experimental apparatus by Teral Inc..

Nomenclature

A	Reference area [m^2]	V_{mer}	Meridional velocity [m/s]
D_c	Casing diameter [m]	V_{θ}	Tangential velocity [m/s]
D_h	Hub diameter [m]		
ΔP	Total pressure-rise [Pa]	ϕ	Flow coefficient [-]
P_T	Total pressure [Pa]	η	Efficiency [-]
Q	Volumetric flow rate [m^3/s]	ρ	Density of air [kg/m^3]
r	Radius [m]	τ	Power coefficient [-]
T	Torque [Nm]	ω	Angular velocity [1/s]
U_t	Reference velocity [m/s]	ψ	Energy coefficient [-]

References

[1] Inoue, M., Ikui, T., Kamada, Y. and Tashiro, M., 1980, "A Quasi Three-Dimensional Design of Diagonal Flow Impellers by Use of Cascade Data," Proceeding of 10th Symposium of IAHR, IAHR, pp. 403-414.

[2] Inoue, M., Ikui, T., Kamada, Y. and Tashiro, M., 1979, “A Design of Axial-Flow Compressor Blades with Inclined Stream Surface and Varying Axial Velocity,” Transaction of Japan Society of Mechanical Engineers, Series B, Vol. 45, No. 389, pp. 11-19.
[3] Ikui, T., Inoue, M., Kamada, Y. and Tashiro, M., 1974, “Improvement and Extension of Carpet Diagram for NACA65 Series Compressor Blades,” Turbomachinery, Vol. 2, No. 5, pp. 444-450.
[4] Kaneko, K., Setoguchi, T. and Inoue, M., 1991, “Passive Control of Unstable Characteristics of a High Specific Speed Diagonal-Flow Fan by an Annular Wing,” Transactions of the ASME, Journal of Turbomachinery, Vol. 113, No. 3, pp. 703-709.
[5] Furukawa, M., Saiki, K., Nagayoshi, K., Kuroumaru, M. and Inoue, M., 1998, “Effects of Stream Surface Inclination on Tip Leakage Flow Fields in Compressor Rotors,” Transactions of the ASME, Journal of Turbomachinery, Vol. 120, No. 4, pp.683-694.
[6] Maeda, H., Sawamura, K. and Miyabe, M., 2010, “Unsteady Flow due to Cavitation in Mixed Flow Pumps,” Proceeding of 3rd Asian Joint Workshop on Thermophysics and Fluid Science, pp. 226-231.
[7] Sawamura, K., Maeda, H., Miyabe, M., Fukuma, T. and Takao, M., 2010, “The effect of Swept-Blade on Cavitation Intensity in Mixed Flow Pumps,” Proceeding of 3rd Asian Joint Workshop on Thermophysics and Fluid Science, pp. 216-221.
[8] Novak, R. A., 1967, “Streamline Curvature Computing Procedures for Fluid-Flow Problems,” Transactions of the ASME, Journal of Engineering for Power, ser. A, Vol. 89, No. 4, pp. 478-490.
[9] Kuroumaru, M., Inoue, M., Higaki, T., Abd-elaziz, F. A. and Ikui, T., 1982, “Measurement of Three-Dimensional Flow Field behind an Impeller by Means of Periodic Multi-Sampling of a Slanted Hot Wire,” Bulletin of the JSME, Vol. 25, No. 209, pp. 1674-1681.

Table 1 Specifications of fan

Energy coefficient, Ψ (Total pressure)		0.647 (1300Pa)
Flow coefficient, Φ (Flow rate)		0.265 (0.805kg/s)
Rotational speed, N		3600 min^{-1}
Vortex pattern		Free vortex
Rotor	Number of blades	6
	Maximum blade thickness / chord	Tip:5% , Hub:10%
	Blade profile	NACA65
Blockage factor		0.96
Inclination angle		Casing:45°, Hub:50°
Tip clearance		0.75 mm
Specific speed (Type number)		670 [min^{-1},m^3/min,m] (1.63)

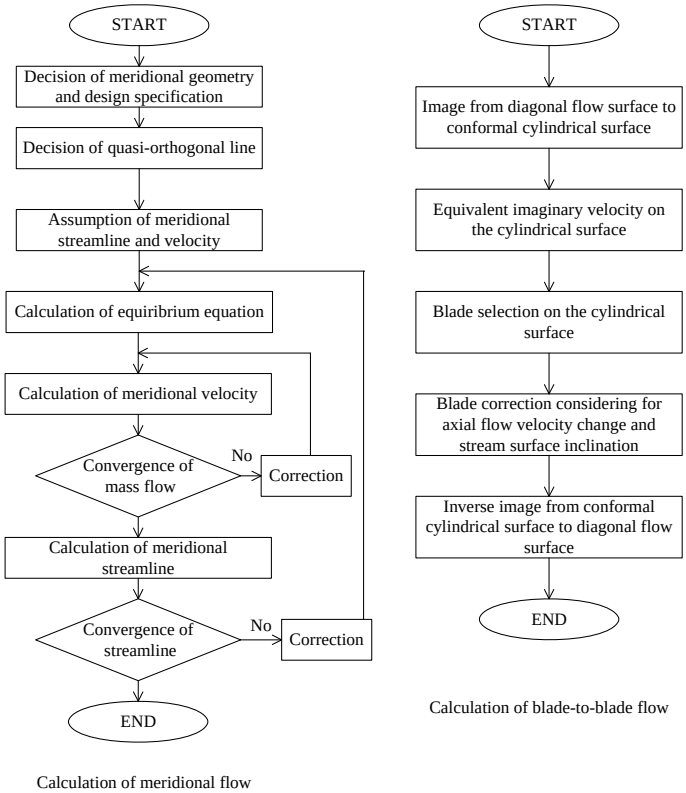

Fig. 1 Design procedure of blade element

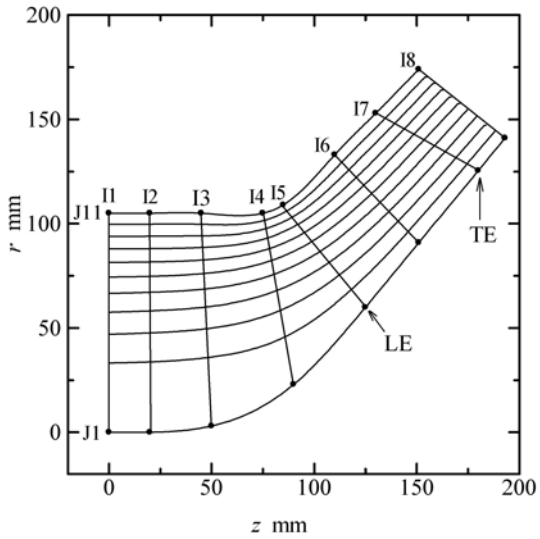

Fig. 2 Meridional streamline

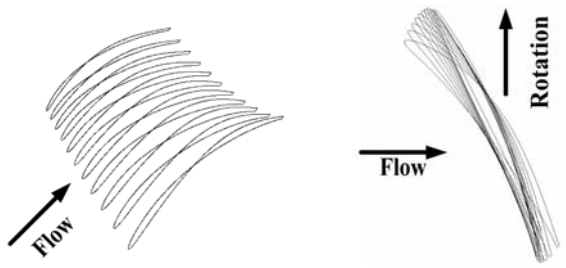

(a) side view (b) top view

Fig. 3 Blade geometery

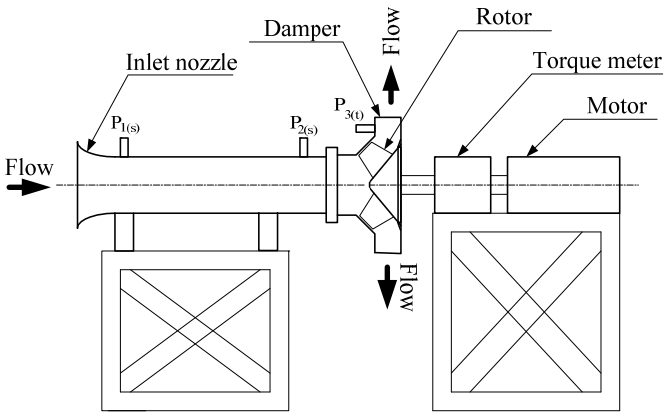

Fig. 4 Experimental apparatus

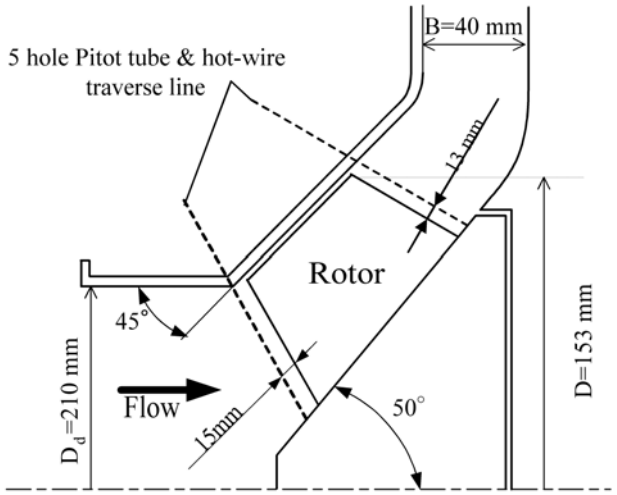

Fig. 5 Outline of fan

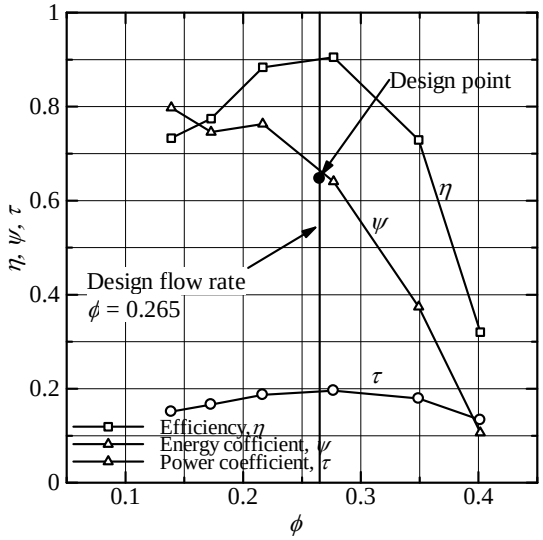

Fig. 6 Fan characteristics

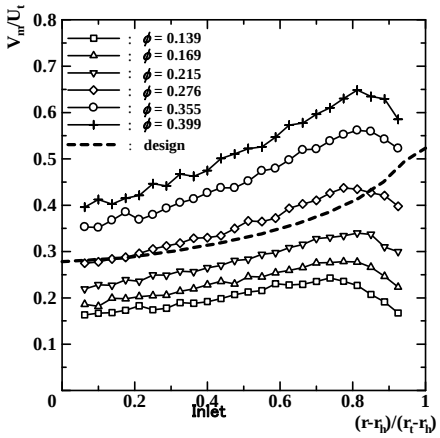

(a) Meridional velocity

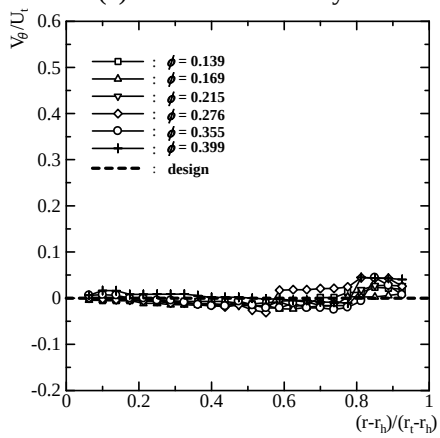

(b) Tangential velocity

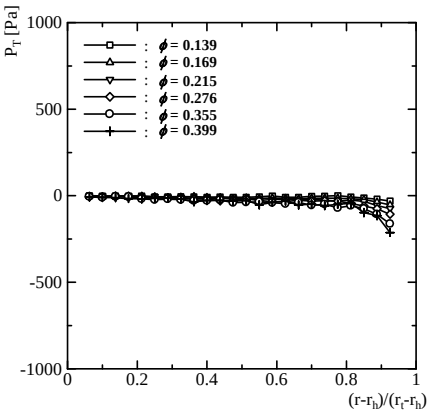

(c) Total pressure

Fig. 7 Flow survey results at rotor inlet by five-hole probe

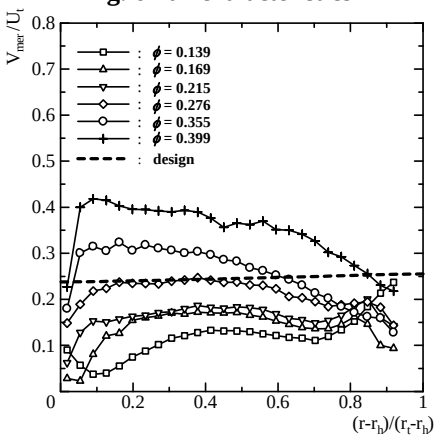

(a) Meridional velocity

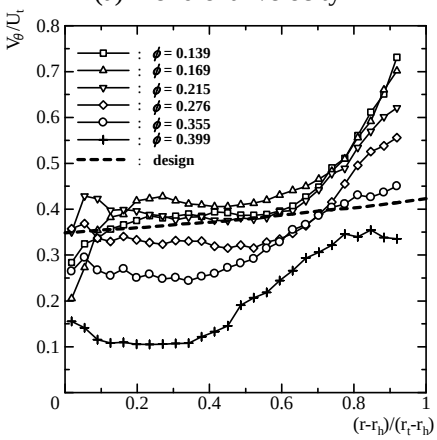

(b) Tangential velocity

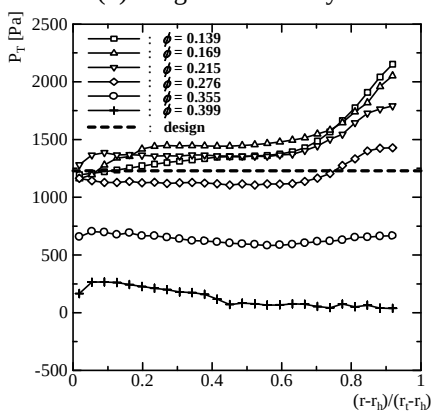

(c) Total pressure

Fig. 8 Flow survey results at rotor outlet by five-hole probe

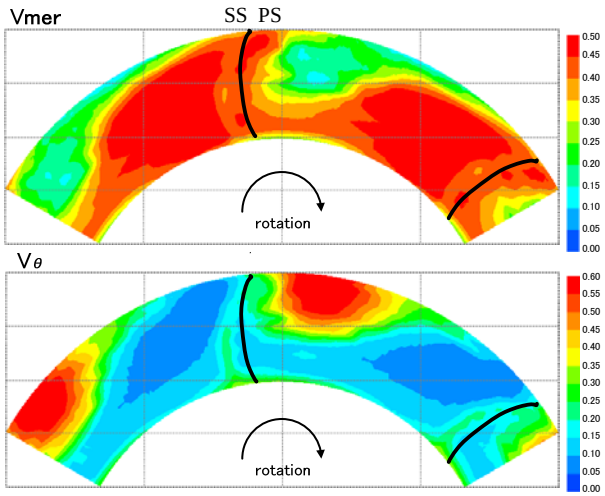

Fig. 9 Contour maps of normalized velocity at rotor outlet by hot-wire probe survey for ϕ=0.399

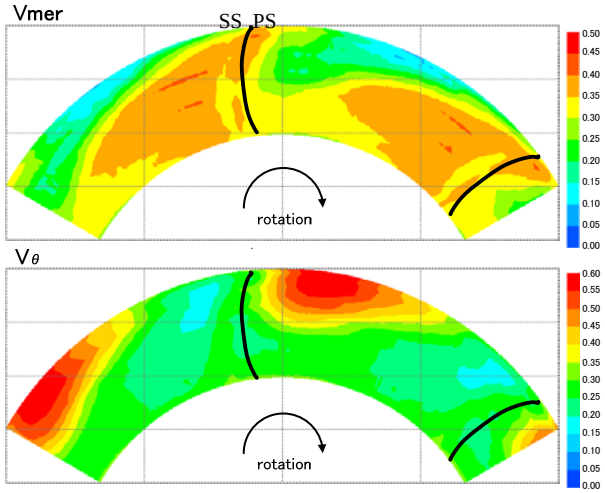

Fig. 10 Contour maps of normalized velocity at rotor outlet by hot-wire probe survey for ϕ=0.355

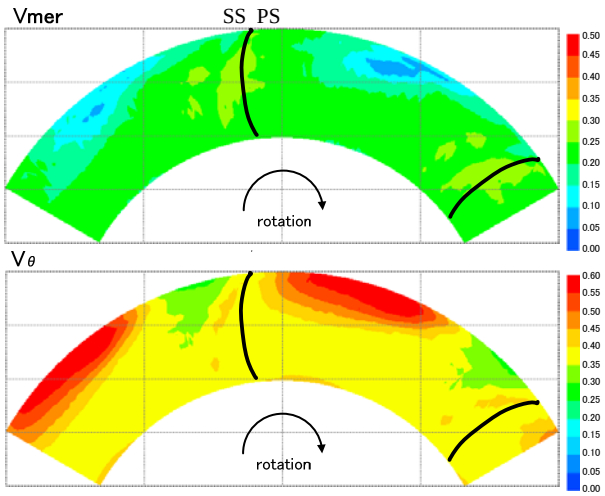

Fig. 11 Contour maps of normalized velocity at rotor outlet by hot-wire probe survey for ϕ=0.276

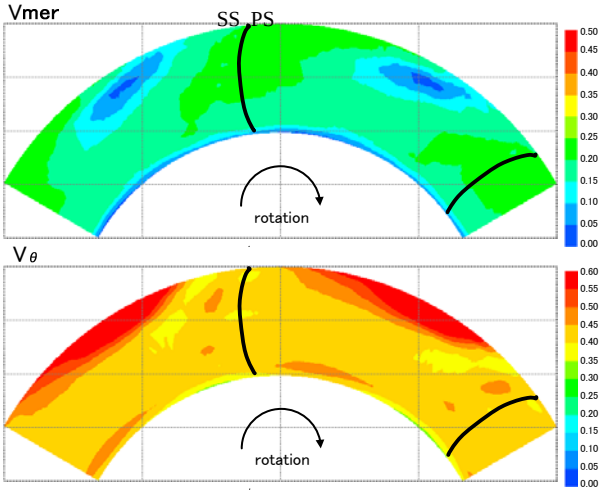

Fig. 12 Contour maps of normalized velocity at rotor outlet by hot-wire probe survey for ϕ=0.215

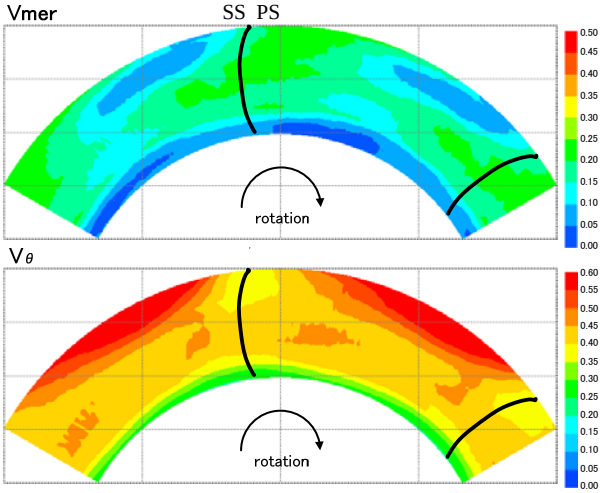

Fig. 13 Contour maps of normalized velocity at rotor outlet by hot-wire probe survey for ϕ=0.169

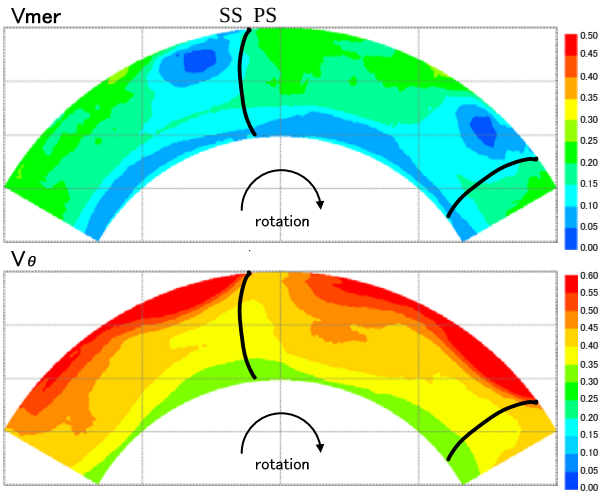

Fig. 14 Contour maps of normalized velocity at rotor outlet by hot-wire probe survey for ϕ=0.139